Chinese Journal of Chemistry, **2009**, *27*, 1929—1936 **Full Paper**

Synthesis of *p*-Nitro-stilbene Derivatives with Different Linking Bonds: An Attempt to Tune Spectroscopy of Dyes with Molecular Engineering

GAO, Fang*(高放) YANG, Liufeng(杨刘峰) WANG, Jianchao(王建超)
XU, Xiaofang(徐晓芳) LI, Hongru*(李红茹) ZHANG, Shengtao*(张胜涛)

College of Chemistry and Chemical Engineering, Chongqing University, Chongqing 400044, China

The synthesis, characterization and spectroscopy of a range of novel substituted *p*-nitro-stilbene derivatives with different bridging bonds were presented. The molecular structure characterization was carried out with ^{1}H NMR, ^{13}C NMR and elemental analysis. The ultraviolet/visible spectroscopy and photoluminescence of the compounds were investigated in various solvents. The maximal absorption wavelength of the nitro-stilbene derivatives with an ether bond exhibited approximate 30 to 40 nm bathochromic shift compared to that of nitro-stilbene dyes with an ester bond. Furthermore, the nitro-stilbene derivatives with an ether bond displayed obvious photoluminescence, while the nitro-stilbene derivatives with an ester bond showed weak fluorescence emission. The detection of the cyclic voltammograms of the nitro-stilbene derivatives showed that the nitro-stilbene compounds with different linking bonds exhibited different redox proceses at various scan rates. The theroretical calculations of HOMO and LUMO energy of nitro-stilbene derivatives showed that the energy gaps between HOMO and LUMO of **3** and **4** were lower than those of **1** and **2**. The electron density of the frontier orbitals of nitro-stilbene derivatives was observed to be affacted by the linking bonds, which thus made it possible to tune the spectroscopy of these dyes with chemical strategy. The differential scanning calorimetry and thermogravimetry showed that the thermal stabilities of these dyes were not much affected by the linking bond. The results presented in this paper would be great interest in development of ideal nitro-stilbene derivatives for special purposes.

Keywords synthesis, spectroscopy, tuning, nitro-stilbene, electrochemistry, molecular geometry optimization

Introduction

Development of photoluminescent and electroluminescent devices, and dye-sensitized solar cells has stimulated the design and synthesis of various functional organic dyes, which has been a particular subject of numerous studies in the past decades.[1-3] The dyes with donor-acceptor and donor-donor structures have been attracted intensive attention because they displayed excellent photophysics and chemical stability.[4-8] In general, electron-donating and electron-accepting groups are constructed to such functional dyes via a π conjugated linker. The spectroscopic properties of organic dyes were found to have strong dependence on the intramolecular charge transfer, which can be mediated by the substituents.[9-11] As a consequence, it was feasible to obtain the dyes with ideal spectroscopy via tuning the intramolecular charge transfer of dyes, which was achived by the decrease of the energy gap between the frontier orbitals of the compounds.

Stilbene dyes have been used in a wide variety of applications such as photoswitable, photochromic, power limiting, non-linear optical materials and so on.[12-15] Modification on the substitutents or conjugation length was performed to obtain long-wavelength and high luminescence efficiency of nitro-stilbene dyes.[16-18] While to date, few reports on the design of short-wavelength absorption of nitro-stilbene dyes were published. In other words, the increase of the energy gap between the frontier orbitals of dyes was seldom reported. This article has been concentrated on the investigation of a series of nitro-stilbene derivatives with different linking bonds in order to tune their spectroscopy (blue-shift or red-shift absorption, weak or strong fluorescence emission). Ester and ether linking bonds were employed to tune the frontier orbital energies of nitro-stilbene derivatives so that the spectroscopy could be tuned. Furthermore, we have investigated the effects of linkage bond on the electrochemistry, electron distribution of frontier orbitals, differential scanning calorimetry (DSC)

* E-mail: fanggao1971@gmail.com
Received February 12, 2009; revised April 2, 2009; accepted May 14, 2009.
Project supported by the the National Natural Science Foundation of China (Nos. 20776165, 20702065, 20872184), Natural Science Foundation of Chongqing Science and Technology Commission (Nos. CSTC 2007BB4175, 2007BB4179) and Key Foundation of Chongqing Science and Technology Commission (Nos. CSTC 2008BA4020, 2009BB4216), A Foundation for the Author of National Excellent Doctoral Dissertation of PR China (No. 200735), the Scientific Research Foundation for the Returned Overseas Chinese Scholars, State Education Ministry (Nos. 20071108-1, 20071108-5), Chongqing University Postgraduates' Science and Innovation Fund (No. 200904A1A0010304).

and thermogravimetry (TG) of nitro-stilbene derivatives.

Experimental

Material

The chemicals and reagents were purchased from Chongqing Medical and Chemical Corporation unless otherwise specified. The organic solvents were dried using standard laboratory techniques according to published methods.[19] The starting materials were further purified with redistillation or recrystallization before use. Compounds **1** to **4** (Figure 1) were synthesized in our laboratory.

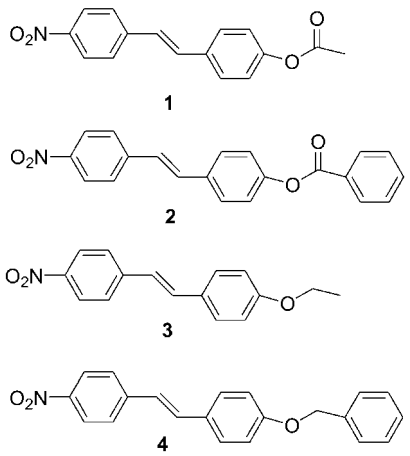

Figure 1 Chemical structures of nitro-stilbene derivatives.

Instruments

UV/visible absorption spectra were recorded with a Cintra spectrophotometer. Emission spectra were determined with a Shimadzu RF-531PC spectrofluorophotonmeter. Quinine sulfate in 0.5 mol•L^{-1} H_2SO_4 (Φ =0.546, 1×10^{-6}—1×10^{-5} mol•L^{-1})[20] was used as a reference to measure the fluorescence quantum yields of the compounds herein. The melting point was detected using a Beijing Fukai melting point apparatus, which was uncorrected. Nuclear magnetic resonance (NMR) spectroscopy was done at room temperature on a Bruker 500 MHz apparatus with tetramethylsilane (TMS) as an internal standard and $CDCl_3$ as solvent. Elemental analysis was conducted by a CE440 elemental analysis meter from Exeter Analytical Inc.

The fluorescence quantum yields of the compounds in solvents with different polarities were measured based on the following equation:[21,22]

$$\Phi_f = \Phi_f^0 \frac{n_0^2 A^0 \int I_f(\lambda_f)\mathrm{d}\lambda_f}{n^2 A \int I_f^0(\lambda_f)\mathrm{d}\lambda_f}$$

where n_0 and n are the refractive indices of the solvents, A^0 and A are the optical densities at excition wavelength, Φ_f and Φ_f^0 are the quantum yields, and the integrals denote the area of the fluorescence bands for the reference and sample, respectively.

Molecular geometry optimization

Geometry optimization calculation was performed with Gaussian 03 package. The density-functional theory (DFT) calculation method and the configuration interaction with single excitation (CIS) method were used to optimize the geometries of the ground state (S_0) and the excited state respectively and energy calculations.[23,24] 6-31G** has been employed as the basis set of all calculations.

Electrochemistry

Electrochemical measurements were carried out using a Shanghai Chenhua working station. Two Pt working electrodes and a Ag/Ag^+ reference electrode, *i.e.* a three-electrode system, were included in a cell. Typically, a 0.05 mol•L^{-1} solution of tetra-*n*-butylammonium hexafluorophosphate in CH_2Cl_2 containing the sample was bubbled with argon for 15 min. The scan rate was 0.1 V•s^{-1} for CV measurements.

Thermal analysis

The differential scanning calorimetry (DSC) and thermogravimetry (TG) were conducted under N_2 flow on a Shimadzu DTG-60H instrument at heating rate 10 ℃•min^{-1}.

Synthesis of nitro-stilbene derivatives

Synthesis of compounds **1** to **4** is shown in Figure 2. *p*-Nitro-*p'*-hydroxyl-stilbene was prepared according to a published method.[25]

***p*-Acetoxy-*p'*-introstilbene** (**1**) *p*-Nitro-*p'*-hydroxyl-stilbene (1.5 g, 6.2 mmol) and triethylamine (TEA) (2.5 g, 24.9 mmol) were dissolved in 100 mL of dry THF. Acetic anhydride (1.9 g, 18.6 mmol) was dropped slowly to the mixture. The resulting mixture was stirred at room temperature under argon for 24 h. The solid was got rid of solution by filtration and the solvents were removed fully by evaporation. The resulting mixture was dissolved in $CHCl_3$ and washed by water for three times. The organic layer was dried with anhydrous sodium sulfate and then concentrated. The product was purified by column chromatography. Further purification was carried out with twice recrystallization from benzene to yield 0.9 g (3.2 mmol) of light yellow compound **1**, yield 52%, m.p. 165.0—165.5 ℃. ^{1}H NMR ($CDCl_3$, 500 MHz) δ: 2.32 (s, 3H, CH_3), 7.10 (d, J= 16.5 Hz, 1H, CH), 7.13 (d, J=8.5 Hz, 2H, Ar-H), 7.23 (s, 1H, CH), 7.56 (d, J=8.5 Hz, 2H, Ar-H), 7.63 (d, J= 9.0 Hz, 2H, Ar-H), 8.22 (d, J=8.5 Hz, 2H, Ar-H); ^{13}C NMR ($CDCl_3$, 125 MHz) δ: 20.668, 121.549, 123.842, 127.481, 128.019, 131.426, 133.968, 143.674, 146.980, 150.996, 168.220. Anal. calcd for $C_{16}H_{13}NO_4$: C 67.84, H 4.63, N 4.94; found C 68.10, H 4.56, N 4.87.

***p*-Benzoyloxy-*p'*-introstilbene** (**2**) *p*-Nitro-*p'*-hydroxyl-stilbene (1.5 g, 6.2 mmol) and triethylamine (TEA) (2.5 g, 24.9 mmol) were dissolved in 200 mL of

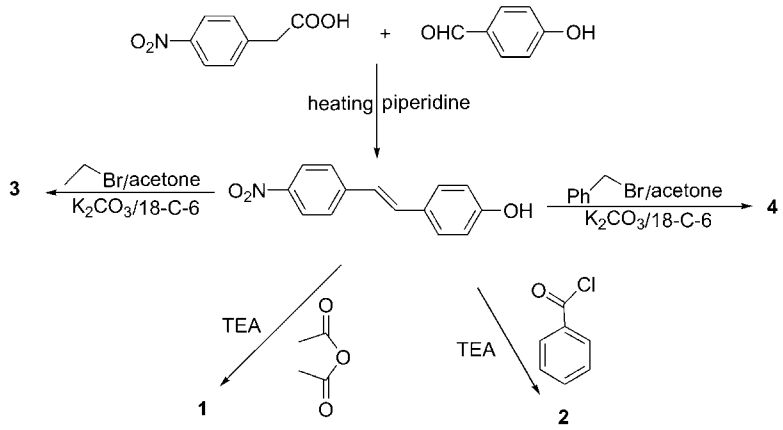

Figure 2 Synthesis route of nitro-stilbene derivatives.

dry THF. Benzyl chloride (2.6 g, 18.6 mmol) was dropped slowly, and the mixture was stirred at room temperature under argon for 24 h. The solid was got rid of solution by filtration and the solvents were removed fully by evaporation. The resulting mixture was dissolved in $CHCl_3$ and washed by water for three times. The organic layer was dried with anhydrous sodium sulfate and then concentrated. The product was purified by column chromatography. Further purification was carried out with twice recrystallization from benzene to yield 1.0 g of modest yellow compound **2** (2.9 mmol), yield 48%, m.p. 227.0—228.5 ℃. ^{1}H NMR ($CDCl_3$, 500 MHz) δ: 7.13 (d, J=16.0 Hz, 1H, CH), 7.26—7.31 (m, 4H, Ar-H, CH), 7.54 (t, J=7.8 Hz, 2H, Ar-H), 7.61—7.68 (m, 4H, Ar-H), 8.23 (t, J=7.8 Hz, 4H, Ar-H); ^{13}C NMR ($CDCl_3$, 125 MHz) δ: 2.258, 124.188, 126.898, 128.093, 128.674, 129.341, 130.219, 132.288, 133.775, 134.033, 143.702, 146.849, 151.281, 165.054. Anal. calcd for $C_{21}H_{15}NO_4$: C 73.03, H 4.38, N 4.06; found C 72.87, H 4.36, N 4.11.

***p*-Ethoxy-*p'*-nitrostilbene (3)** 2.0 g (8.3 mmol) of *p*-nitro-*p'*-hydroxyl-stilbene and bromoethane (1.3 g, 12.4 mmol) were dissolved in 150 mL of dried acetone. Anhydrous potassium carbonate (2.3 g, 16.6 mmol) and a few drops of 18-C-6 were added to the solution. The reactant mixture was stirred at room temperature under argon for 24 h. The solid was got rid of solution by filtration and THF was removed fully by evaporation. The resulting mixture was dissolved in $CHCl_3$ and washed by water for three times. The organic layer was dried with anhydrous sodium sulfate and then concentrated. The product was purified by column chromatography. Further purification was carried out with twice recrystallization from benzene to yield 1.0 g (3.7 mmol) golden yellow compound **3**, yield 45%, m.p. 143—144 ℃. ^{1}H NMR ($CDCl_3$, 500 MHz) δ: 1.44 (t, J=7.0 Hz, 3H, CH_3), 4.05—4.09 (m, 2H, CH_2), 6.91 (d, J=9.0 Hz, 2H, Ar-H), 6.99 (d, J=16.5 Hz, 1H, CH), 7.21 (d, J=16.5 Hz, 1H, CH), 7.48 (d, J=9.0 Hz, 2H, Ar-H), 7.58 (d, J=8.5 Hz, 2H, Ar-H), 8.19 (d, J=8.5 Hz, 2H, Ar-H); ^{13}C NMR ($CDCl_3$, 125 MHz) δ: 14.791, 63.590, 114.862, 123.955, 126.471, 128.430, 128.792, 132.986, 144.345, 146.389, 159.667. Anal. calcd for $C_{16}H_{15}NO_3$: C 71.36, H 5.61, N 5.20; found C 71.76, H 5.51, N 5.12.

***p*-Benzyloxy-*p'*-introstilbene (4)** 2.0 g (8.3 mmol) of *p*-nitro-*p'*-hydroxyl-stilbene and benzyl bromide (2.1 g, 12.4 mmol) were dissolved in 100 mL of dried acetone. Anhydrous potassium carbonate (2.3 g, 16.6 mmol) and a few drops of 18-C-6 were added to the solution. The mixture was stirred at room temperature under argon for 24 h. The solid was got rid of solution by filtration and THF was removed fully by evaporation. The resulting mixture was dissolved in $CHCl_3$ and washed by water for three times. The organic layer was dried with anhydrous sodium sulfate and then concentrated. The product was purified by column chromatography. Further purification was carried out with twice recrystallization from benzene to yield 1.1 g (3.32 mmol) of deep yellow compound **4**, yield 41%, m.p. 197—198 ℃. ^{1}H NMR ($CDCl_3$, 500 MHz) δ: 5.11 (s, 2H, CH_2), 7.01 (t, J=7.8 Hz, 3H, Ar-H, CH), 7.22 (d, J=16.5 Hz, 1H, CH), 7.34 (t, J=7.6 Hz, 1H, Ar-H), 7.40 (t, J=7.5 Hz, 2H, Ar-H), 7.45 (d, J=7.0 Hz, 2H, Ar-H), 7.50 (d, J=8.5 Hz, 2H, Ar-H), 7.60 (d, J=8.5 Hz, 2H, Ar-H), 8.20 (d, J=8.5 Hz, 2H, Ar-H); ^{13}C NMR ($CDCl_3$, 125 MHz) δ: 70.105, 115.278, 124.159, 126.522, 127.473, 128.119, 128.440, 128.659, 129.219, 132.864, 136.636, 144.263, 146.451, 159.441. Anal. calcd for $C_{21}H_{17}NO_3$: C 76.12, H 5.17, N 4.23; found C 75.93, H 5.12, N 4.56.

Results and discussion

Synthesis and structural characterization of the compounds

Synthesis of compounds **1** to **4** (Figure 1) was performed with a routine route. Owing to electron-withdrawing of nitro group and conjugation effect of *p*-nitro-*p'*-hydroxyl-stilbene, the hydroxyl group displayed excellent reactivity. The condensation reaction of *p*-nitro-*p'*-hydroxyl-stilbene with halide easily occurred in a mild condition. Although the single crystals of these compounds were not obtained in various solvents, we got very pure compounds with flash chromatography and recrystallization. Clean ^{1}H NMR and ^{13}C NMR

spectra as well as narrow-range melting temperature of the comounds were obtained.

Spectroscopic properties

UV-visible spectroscopy The optical data of these compounds are listed in Table 1. Dramatic difference in the maximal absorption wavelength is observed for compounds **1** to **4**. A typical comparison of UV/visible absorption spectroscopy of compound **1** with compound **3** in methyl chloride is shown in Figure 3. As compared with compounds **3** and **4**, compounds **1** and **2** exhibited approximate 40 nm blue-shift in the maximal absorption wavelength in methyl chloride. It was evident that the absorption wavelength of nitro-stilbene could be efficiently tuned by the linking bond.

The maximal absorption wavelength of the nitro-stilbene dyes with an ester linking bond displayed weak solvent effect. While in contrast, the nitro-stilbene dyes with an ether linking bond showed remarkable solvent effect, which suggested that the linking bond played an important role in the absorption spectroscopy of the nitro-stilbene derivatives. The ester bridging bond diminished the intramolecular charge transfer due to its electron deficiency effect. While in contrast, the ether linking bond enhanced intramolecular charge transfer because of its electron-donating effect. A change from donor-π-acceptor to acceptor-π-acceptor occurred with the introduction of the ester bond, which led to the reduction in the intramolecular charge transfer. A sketch of molecular structures of compounds **2** and **4** is shown in Figure 4. As a result, the absorption spectroscopy of nitro-stilbene derivatives was efficiently tuned. The maximal absorption wavelength of single molecular electronic spectroscopy of compounds **1** to **4** in vacuum was calculated, and the results are listed in Table 1. The calculated results were similar to the experimental observation, indicating that intramolecular charge transfer played a key role in the maximal absorption wavelength. The results showed the photophysical significance of the electropositivity of the substituents and the consequences for the π-π* and n-π* transitions of the compounds. The calculations with a density-functional theory (DFT) method on the dipole moments of the ground state (Table 1) demonstrated that compounds **3** and **4** had higher dipole moments than those of compounds **1** and **2**.

Fluorescence spectroscopy Compounds **1** and **2** displayed weak fluorescence emission in various solvents. While in contrast, compounds **3** and **4** exhibited strong fluorescence emission in modest polar solvents such as ethyl acetate and THF. This indicated that the linking bond had significant effects on the fluorescence spectroscopy of nitro-stilbene derivatives. A typical comparison of fluorescence spectroscopy of compound **1** with **3** in methyl chloride is shown in Figure 5, which clearly showed that fluorescence intensity of compound **1** was remarkably lower than that of compound **3**. Similar phenomenon was found for compounds **2** and **4**. The electron deficiency effect of ester linking bond suppressed the fluorescence emission of nitro-stilbene derivatives at the long-wavelength (500—700 nm). While in contrast, their fluorescence emission could be increased by the electron-donating effect of ether bridged bond. The fluorescence quantum yields of compounds **1** to **4** in various solvents are presented in Table 2. Dramatically different fluorescence quantum yields were found for these nitro-stilbene derivatives. Itoh *et al.* have pointed out that ester bond could increase the intersystem crossing coefficients of some organic molecules from singlet state to triplet state, which resulted in low fluorescence emission.[26] In the present study, **1** and **2** could be characterized with high intersystem crossing coefficients as well due to the effect of ester bond. As a consequence, the fluorescence quantum yields of nitro-stilbene derivatives with ester linking bond could be highly reduced. Generally, intramolecular charge transfer is weak in low-polar solvents. Hence, compounds **3** and **4** displayed week fluorescence in non-polar solvent such as cyclohexane. On the other hand, the maximal emission wavelength displayed red-shift in polar solvents because they exhibited intramolecualr charge transfer to more extent in polar solvents. Photoisomerization and torsion of double bond might lead to decrease of the fluorescence emission of compounds **3** and **4** in very strong polar solvents such as acetonitrile

Table 1 Absorption spectral data of compounds **1** to **4** in various solvents [a]

Solvent	λ_{max}/nm				ε/(10^5 L•mol^{-1}•cm^{-1})			
	C1	C2	C3	C4	C1	C2	C3	C4
Cyclohexane	335	334	353	352	0.156	0.109	0.176	0.156
Benzene	341	341	367	367	0.180	0.233	0.130	0.123
Ethyl acetate	335	333	361	360	0.144	0.250	0.124	0.141
THF	336	338	380	379	0.256	0.132	0.168	0.172
CH_2Cl_2	344	345	380	380	0.146	0.146	0.255	0.274
CH_3CN	343	343	373	373	0.147	0.117	0.295	0.276
Calculated[a]	334	351	381	377			—	
Dipole moment[a]	7.121	7.934	8.919	8.092			—	

[a] For single molecule in vacuum, not real data in solvents; Diople moment: Derby, in vacuum.

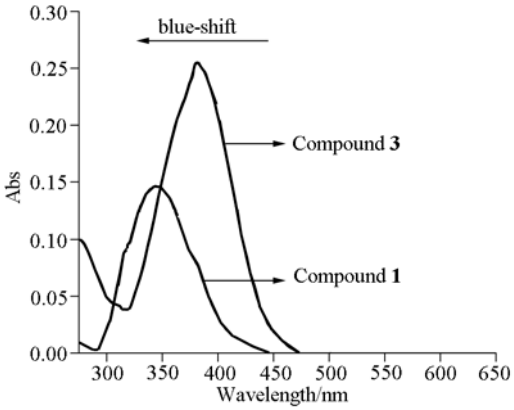

Figure 3 Typical absorption spectroscopy of compounds **1** and **3** in methyl chloride (1×10^{-5} mol•L^{-1}).

and DMF.[27,28]

Electrochemistry

The cyclic voltammograms of the compounds **1** to **4** were recorded in methyl chloride from 50 to 150 mV•s^{-1} as shown in Figure 6. Obviously, the redox process of compound **1** was characterized by irreversible property. Three reduction peaks (−0.669, −1.301, −1.571 V) were found at all sweep rates in the negative region at a scan rate 100 mV•s^{-1}. And two oxidation peaks (−0.201 and 0.112 V) were observed at the scan rate 100 mV•s^{-1}. No corresponding redox peaks were found at all scan rates. While for the redox process, the peak currents increased linearly with the square root of scan rates, suggesting diffusion-controlled electron transfer reactions.

The cyclic voltammetry of compound **2** displayed four reduction peaks at 100 mV•s^{-1} sweeping rate. Three reduction peaks were obtained in the negative region: −0.191, −1238, −1.439 V. One oxidation peak was got in the positive region: 0.580 V. The redox process of compound **2** was dominated by diffusion-controlled electron transfer reactions resulting from linear increasing of peak currents with the square root of scan rates.

Figure 6(c) showed typical cyclic voltammograms of compound **3** at different scan rates. One reduction peak at −1.232 V and two oxidation peaks at −0.178, 1.223 V were observed at scan rate 100 mV•s^{-1}. Obviously, the reduction peaks and oxidation peaks could not be regarded as the corresponding redox couples. Linear increasing of peak currents with the square root of scan rates suggested that the redox process of compound **3** was controlled by diffusion-controlled electron transfer reactions.

Typical cyclic voltammograms of compound **4** at different scan rates were shown in Figure 6(d). No pair peaks were observed at all scan rates. Only one reduction peak was found in negative region at −1.558 V, and the oxidation peaks were observed in positive region 1.031 and 1.268 V at scan rate 100 mV•s^{-1}. The peak currents showed linear increasing with the square root of scan rates, which indicated that redox process of compound **4** was dominated by the diffusion-controlled electron transfer reaction.

Clearly, compounds **1** and **2** displayed more complicated redox processes at various scan rates than compounds **3** and **4**, although all redox processes of these compounds were characterized with irreversible nature. Compounds **1** and **2** exhibited three similar reduction potentials in the negative region. In contrast, the only one reduction potential of compounds **3** and **4** was much like. Nitro group is powerful electron-withdrawing species in compounds **1** to **4** and the occurrence of its reduction reaction could be easily observed.[29] Likewise, we would expect that an ester group in the compounds **1** and **2**, as an electron-withdrawing group, could undergo reduction process as well.[30] Furthermore, the electron-withdrawing effects of nitro group and ester group might decrease the electron density of the double bond of compounds **1** and **2** and thus its reduction could easily take place. Remarkably, as description of the cyclic voltammograms of compounds **1** to **4**, the results were ture that more reduction peaks were detected for compounds **1** and **2** than compounds **3** and **4**, which was consistent with our expection.

The energy calculations of the frontier orbitals of compounds **1** to **4** of ground state S_0 and excited state S_1 were peroformed with Gaussian 03 package and the results are presented in Table 3. The results showed that the erergy gaps of **3** and **4** were smaller than those of **1** and **2**, thus these compounds exhibited remarkably different maximal absorption wavelength. The frontier orbital electron destributions of S_0 and S_1 of compounds **1** to **4** are presented in Figure 7, which clearly showed that the electron density distribution of nitro-stilbene derivatives was affected by the linking bond. This in-

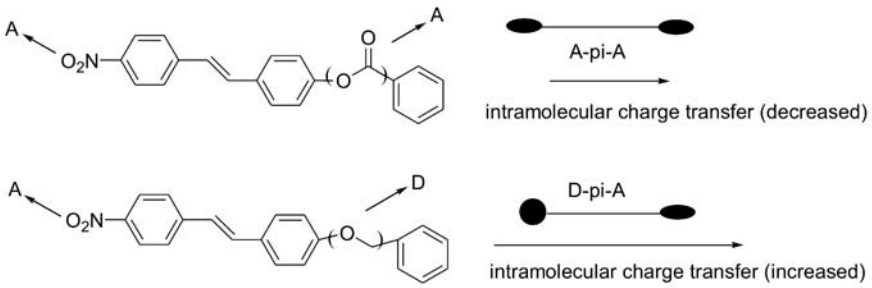

Figure 4 A sketch of intramolecular charge transfer for compounds **2** and **4**.

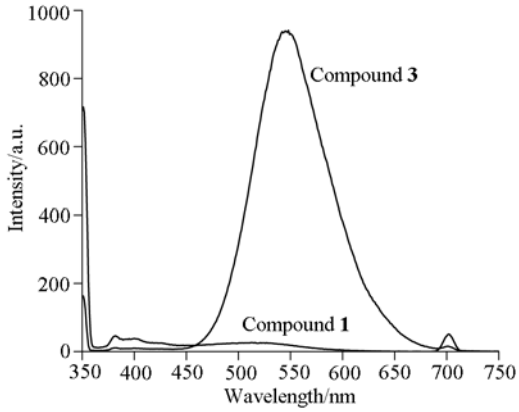

Figure 5 Typical fluorescence spectroscopy of compounds **1** and **3** excited at 350 nm in methyl chloride (1×10^{-6} mol•L^{-1}). Slit of window: Ex: 5 nm, Em: 3 nm.

Table 2 Fluorescence quantum yields of compounds **1** to **4** in various solvents [a]

Solvent	Fluorescence quantum yield			
	1	**2**	**3**	**4**
Cyclohexane	0.0045	0.0084	0.0048	0.0084
Benzene	0.0062	0.0054	0.011	0.018
Ethyl acetate	0.0078	0.0058	0.091	0.088
THF	0.0086	0.0072	0.11	0.090
CH_2Cl_2	0.0072	0.07	0.53	0.34
CH_3CN	0.0094	0.016	0.018	0.026

[a] The error within 10%, five times measurements.

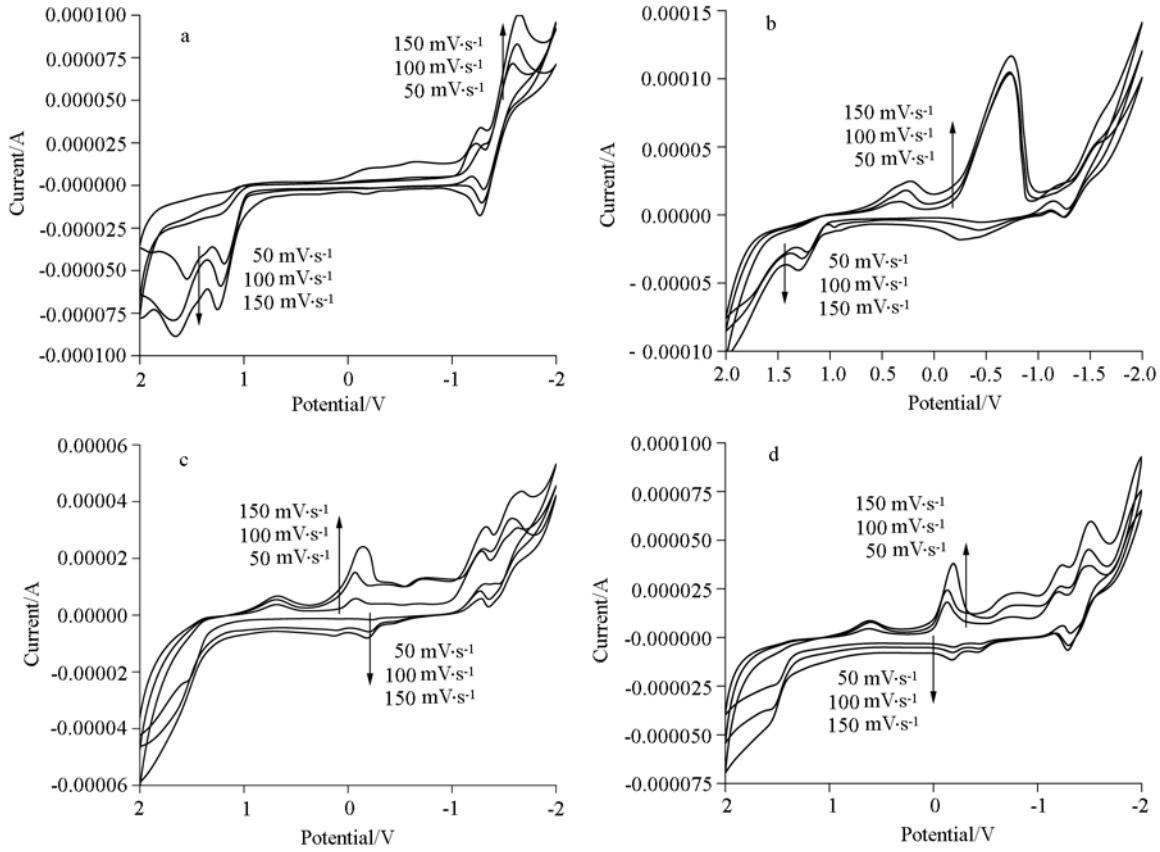

Figure 6 Cyclic voltammograms of compounds **1** (a), **2** (b), **3** (c), **4** (d) at various scan rates (from 50 to 150 mV•s^{-1}).

Table 3 HOMO and LUMO orbital energies (eV) of the ground state S_0 and the excited singlet state S_1 of compounds **1** to **4**

S	**1**		**2**		**3**		**4**	
	HO	LU	HO	LU	HO	LU	HO	LU
S_0	−5.995	−2.567	−6.006	−2.562	−5.669	−2.429	−5.705	−2.446
S_1	−5.716	−2.642	−5.733	−2.648	−5.404	−2.433	−5.410	−2.439

fluence led to the difference in the frontier orbital energies of compounds **1** to **4**, as shown in Table 3. As a consequence, different UV/visible spectroscopy, fluorescence and electrochemical properties of nitro-stilbene derivatives were observed.

Thermal analysis

The analysis of the thermal properties was performed by differential scanning calorimetry (DSC) and thermogravimetric analysis (TGA) under a nitrogen at-

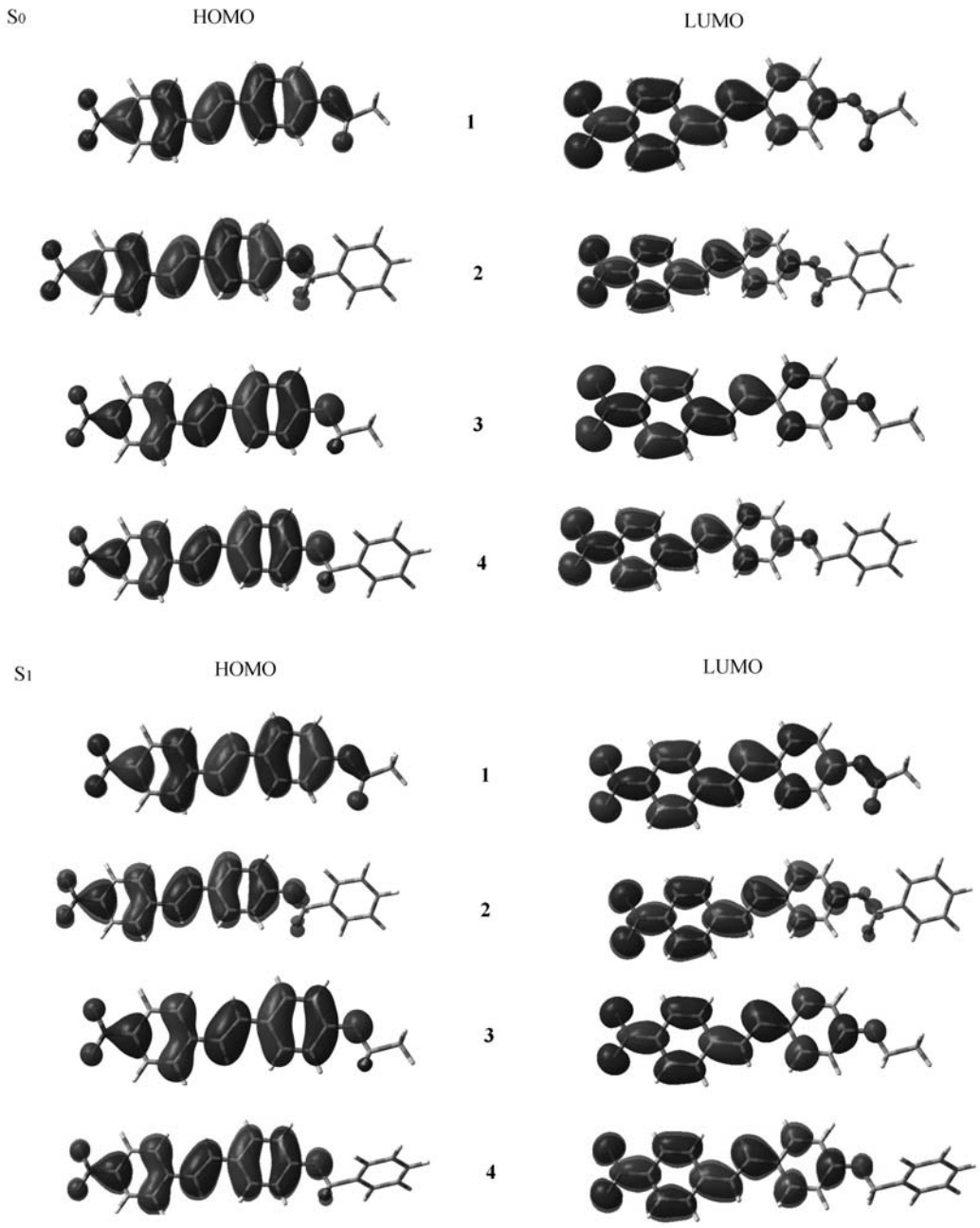

Figure 7 Electron density diagrams of the HOMO and LUMO of the ground state and the excited state of compounds **1** to **4**.

mosphere. The onset decomposition temperatures of compounds **1** to **4** determined by TGA were 334.14, 402.24, 328.00 and 333.82 ℃ respectively as presented in Figure 8, demonstrating that these compounds had good themal stability. The weight loss of **1** (MW＝283.28) was 79.558% at 334.14 ℃, which was close to the loss of nitro-stilbene part (MW＝225.24). Interestingly, the weight loss of **2** (MW＝345.35) was 62.882%, which was also close to the loss of nitro-stilbene part (MW＝225.24). Furthermore, the weight loss of **3** (MW＝269.30) was 81.051%, which was perfectly close to the loss of nitro-stilbene part (MW＝225.24). **4** (MW＝331.36) displayed 35.683% weight loss, which was close to the loss of phenylethyloxyl group (MW＝107.13). The analysis showed that: (1) the decomposition of the compounds **1** to **4** did occur at high temperatures, and (2) the linking bond did not play remarkable effects on the thermal stabilities of nitro-stilbene derivatives.

Conclusion

A number of nitro-stilbene derivatives with different linking bonds were successfully synthesized. The paper presented efficient chemical strategy on tuning the absorption and fluorescence spectroscopy of nitro-stilbene dyes by varying electron-donating or electron-withdrawing bridging bond, which was achieved by the influence of the bridging bond on electron distribution of frontier molecular orbitals of nitro-stilbene deriva-

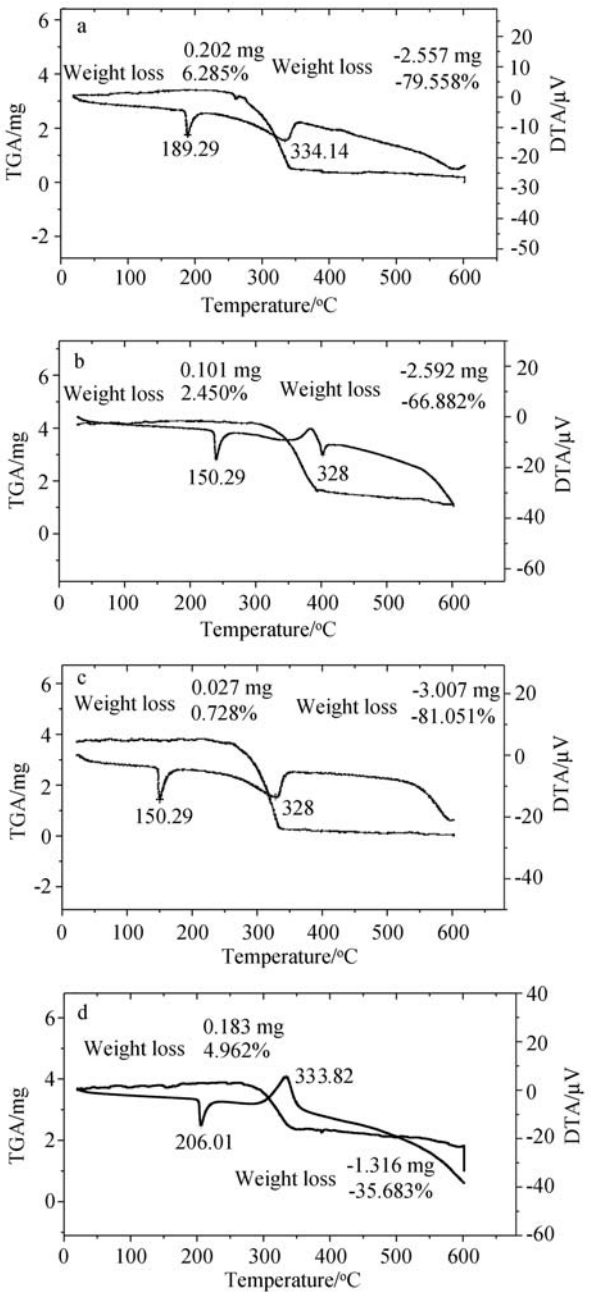

Figure 8 DSC and TGA curves of the compounds **1** (a), **2** (b), **3** (c) and **4** (d).

tives. The electrochemical properties of nitro-stilbene derivatives were thus influenced by the linking bond. The chemical strategy shown herein would be a great approach to the development of various nitro-stilbene derivatives for special aims.

References

1 Song, X.; Wang, B.; Zhang, X.; Li, C.; Wang, X.; Zhang, B. *Acta Chim. Sinica* **2008**, *66*, 1687 (in Chinese).
2 Li, F.; Yu, J.; Zhang, B.; Huang, C. *Acta Chim. Sinica* **2006**, *64*, 301 (in Chinese).
3 Wang, P.; Xie, Z.; Hong, Z.; Tang, J.; Wong, O.; Lee, C.; Wong, N.; Lee, S. *J. Mater. Chem.* **2003**, *13*, 1894.
4 El-Zaria, M. E.; Etaiw, S. H.; Ibrahim, M. S. *Appl. Organomet. Chem.* **2005**, *19*, 1114.
5 Retig, W.; Strehmel, B.; Majenz, W. *Chem. Phys.* **1993**, *173*, 525.
6 Mishra, A.; Behera, G. B.; Krishna, M. M.; Periasamy, G. N. *J. Luminescence* **2001**, *92*, 175.
7 Gerold, J.; Holzenkamp, U.; Meier, H. *Eur. J. Org. Chem.* **2001**, *14*, 2757.
8 Li, D.; Zhao, W.; Sun, X.; Zhang, J.; Anpo, M.; Zhao, J. *Dyes Pigments* **2006**, *68*, 33.
9 Pond, S. J. K.; Rumi, M.; Levin, M. D.; Parker, T. C.; Beljonne, D.; Day, M. W.; Bredas, J. L.; Marder, S. R.; Perry, J. W. *J. Phys. Chem. A* **2002**, *106*, 11470.
10 Pond, S. J. K.; Tsutsumi, O.; Rumi, M.; Kwon, O.; Zojer, E.; Bredas, J. L.; Marder, S. R.; Perry, J. W. *J. Am. Chem. Soc.* **2004**, *126*, 9291.
11 Zhou, Y.; Peng, P.; Han, L.; Tian, W. *Synth. Met.* **2004**, *157*, 502.
12 Zhu, L.; Yi, Y.; Shuai, Z.; Bredas, J.; Beljonne, D.; Zojer, E. *J. Chem. Phys.* **2006**, *125*, 44101.
13 Wang, X.; Wang, D.; Zhou, G.; Yu, W.; Zhou, Y.; Fang, Q.; Jiang, M. *J. Mater. Chem.* **2004**, *11*, 1600.
14 Breitung, E. M.; Shu, C.; McMahon, R. J. *J. Am. Chem. Soc*. **2000**, *122*, 1154.
15 Wang, X.; Zhou, Y.; Yu, W.; Wang, C.; Fang, Q.; Jiang, M.; Lei, H.; Wang, H. *J. Mater. Chem.* **2000**, *10*, 2698.
16 Alami, M.; Liron, F.; Gervais, M.; Peyrat, J. F.; Brion, J. D. *Angew. Chem., Int. Ed* **2000**, *41*, 1578.
17 Fayed, T. A.; Etaiw, S. E. H.; Khatab, H. M. *J. Photochem. Photobiol. A*: *Chem.* **2005**, *170*, 97.
18 Jha, P. C.; Das, M.; Ramasesha, S. *J. Phys. Chem. A* **2004**, *108*, 6279.
19 Perrin, D. D.; Armarego, W. L. F.; Perrin, D. R. *Purification of Laboratory Chemicals*, Pergamon, New York, **1996**.
20 Eaton, D. F. *Pure Appl. Chem*. **1988**, *60*, 1107.
21 Maus, M.; Rettig, W.; Bonafoux, D.; Lapouyade, R. *J. Phys. Chem. A* **1999**, *103*, 3388.
22 Lukeman, M.; Vea, D.; Wa, P.; Ranji, V.; Munasingh, N.; Corrie, J. E. T. *Can. J. Chem.* **2004**, *82*, 240.
23 Fores, M.; Duran, M.; Adamowicz, L. *J. Phys. Chem. A* **1999**, *103*, 4413.
24 Casida, M. E.; Jamorski, C.; Casido, K. C.; Salahub, D. R. *J. Chem. Phys.* **1998**, *108*, 4439.
25 Cavallini, G.; Massarani, E. *US 2878291*, **1959** [*Chem. Abstr*. **1960**, *54*, 97459].
26 Itoh, Y.; Gouki, M.; Goshima, T.; Hachimori, A.; Kojima, M.; Karatsu, T. *J. Photochem. Photobiol.* **1998**, *117*, 91.
27 Gorner, H.; Khun, H. J. *Advances in Photochemistry*, Vol. 19, Eds: Douglas, C. N.; David, H. V.; Günther, von B., John Wiley & Sons, Inc., New York, **2007**.
28 Yang, J. S.; Liau, K. L.; Hwang, C. Y.; Wang, C. M. *J. Phys. Chem. A* **2006**, *110*, 8003.
29 Squella, J. A.; Sturm, J. C.; Weiss-Lopez, B.; Bonta, M.; Nunez-Vergara, L. J. *J. Electroanal. Chem.* **1999**, *466*, 90.
30 Ramesh, P.; Sampath, S. *Analyst* **2001**, *126*, 1872.

(E0902121 Sun, H.)